An Immunocompetent Murine Model of Metastatic Mammary Cancer Accessible to Bioluminescence Imaging

MASA-AKI SHIBATA[1,2], EIKO SHIBATA[2*], JUNJI MORIMOTO[3], NABIL A.S. EID[1], YOSHIHISA TANAKA[1], MASAHITO WATANABE[4] and YOSHINORI OTSUKI[1,2]

[1]Department of Anatomy and Cell Biology, Division of Life Sciences, [2]High-Tech Research Center, and [3]Laboratory Animal Center, Osaka Medical College, Takatsuki, Osaka 569-8686; [4]Osaka Health Science University, Osaka, Osaka 530-0043, Japan

Abstract. *Background: Many areas of research, including gene and pharmacological therapeutics, would benefit from longitudinal in vivo monitoring methodologies. To investigate the feasibility of one such methodology, we developed a murine mammary cancer model amenable to sequential bioluminescent imaging of tumor growth and metastasis in living animals. Materials and Methods: Metastatic mouse mammary carcinoma BJMC3879 cells were transfected to stably express firefly luciferase and inoculated into immunocompetent female BALB/c mice. Results: Sequential analysis using bioluminescent imaging showed increasing photon counts correlated to expanding mammary tumor volumes; in addition, strong signals from axillary, mandibular, femoral, thoracic and abdominal regions in mice were histopathologically determined to be due to metastases, the majority of which occurred in lymph nodes and lungs. Conclusion: The bioluminescent mouse mammary cancer model we established provides a method for quantifiable longitudinal in vivo imaging that can be used in gene and pharmacological therapy applications.*

Abbreviations: CT, computed tomography; GFP, green fluorescence protein; MMTV, mouse mammary tumor virus; MRI, magnetic resonance imaging; PET, positron emission tomography.

**Present address:* Department of Bioscience, National Cardiovascular Center Research Institute, Suita, Osaka 565-8565 Japan

Correspondence to: Dr. M.A. Shibata or Dr. Y. Otsuki, Department of Anatomy and Cell Biology, Division of Life Sciences, Osaka Medical College, 2-7 Daigaku-machi, Takatsuki, Osaka 569-8686, Japan. Tel: +81 726847197, Fax: +81 726846511, e-mail: shibatam@art.osaka-med.ac.jp, or an1000@art.osaka-med.ac.jp

Key Words: Luciferase, bioluminescence imaging, mammary cancer, metastasis.

The ability to detect cancer metastasis and its location(s) in laboratory animals *in vivo* has direct translational relevance to such detection in the human clinical setting. In basic laboratory animal experimentation, biomedical imaging systems can also significantly reduce the number of animals required in longitudinal studies and increase the experimental data harvested for each animal (1). Imaging tools for biomedical research and medicine are rapidly improving and new techniques have been developed within the past decade. Biomedical imaging systems such as ultrasound, magnetic resonance imaging (MRI), computed tomography (CT) and positron emission tomography (PET) have become very important tools in both diagnosis and therapy and provide the means of tracing individual cells and tissues to provide proof of efficacy and agent delivery.

The ability to stably integrate/transfect genes into the genome of mammalian cells is extremely important if the major applications of transfection are the analysis of gene function and regulation, large-scale protein production, and gene therapy. It is equally important to be able to trace these modified cells by means of integrated reporter genes. This has special importance in cancer, where it would be extremely useful to trace such parameters as tumor growth and metastasis. Two of the more commonly used reporter genes are those that code for green fluorescent protein (GFP) and the enzyme luciferase. The *in vivo* use of fluorescing compounds such as GFP in bio-imaging has several limitations, notably autofluorescence of the hair under external illumination, and weak skin penetration of the low-wavelength light produced (2); in addition, an external source light is required for GFP excitation (2). Luciferase, in contrast, is bioluminescent, producing light only upon interaction with its substrate, luciferin.

Although many molecules have been implicated in cancer metastasis, the detailed mechanism of metastasis is still not fully understood. Since breast cancer is the most common malignancy in women, and metastasis is the number one cause

of mortality in this malignancy (3), we sought to establish a comparable mammary cancer system accessible to bioluminescent imaging of tumor growth and metastasis in living animals by using a murine metastatic mammary tumor model in which the tumor cells stably express firefly luciferase.

Materials and Methods

Vectors. luc2, an improved firefly luciferase gene showing strong expression in mammalian cells, was excised from a pGL4.10 vector (Promega, Madison, WI, USA) by digestion with *Nhe*I/*Xba*I. The *luc2* gene fragment was ligated into a *Nhe*I/*Xba*I- digested pTracer-CMV/Bsd plasmid vector containing a gene conferring resistance to blasticidin (Invitrogen, Inc., Carlsbad, CA, USA). The plasmid vector was extracted from *Escherichia coli* (DH5α strain) and initially purified using a modified alkaline lysis procedure and a Qiagen Plasmid Maxi Kit (Qiagen Inc., Valencia, CA, USA), with further purification using centrifugal filters (Ultrafree-MC, Millipore Co., Bedford, MA, USA). The combined vector is referred to as pTracer-Luc2.

Parent mammary tumor cell line. Mouse mammary tumor virus (MMTV), purified from medium in which Jyg-MC cells (established from mammary tumors of the Chinese wild mouse) were grown, was inoculated into the inguinal mammary glands of female BALB/c mice, resulting in the development of mammary carcinomas (4). The BJMC3879 mammary adenocarcinoma cell line was subsequently derived from a metastatic focus within a lymph node from one of the inoculated mice and the cell line continues to show a high metastatic propensity, especially to lymph nodes and lungs (5-7). The BJMC3879 cell line was maintained in either RPMI-1640 medium or Dulbecco's modified Eagle's medium containing 10% fetal bovine serum supplemented with streptomycin/penicillin in an incubator at 37˚C and under a 5% CO_2 atmosphere.

Stable transfection of luciferase gene. BJMC3879 mammary carcinoma cells were subjected to electroporation with the pTracer-Luc2 vector. Transfection was conducted using an amaxa Nucleofector device (amaxa GmbH, Köln, Germany). In the transfection process, BJMC3879 cells (1×10^7) were suspended in 100 μl of Nucleofector V solution (amaxa GmbH) to which 2.5 μg of the pTracer-Luc2 vector were added and gene electrotransfer then conducted using the amaxa Nucleofector system with program number T03. The transfected cells were then plated in T-75 flasks. Three days later, the cells were exposed to 5 μg/ml blasticidin. Medium containing 5 μg/ml blasticidin was changed twice a week for 2 weeks, once a week for 1 week, and changed once a month thereafter. Concentration of the blasticidin in the medium was increased to 10 μg/ml in a stepwise manner at each medium change.

D-Luciferin potassium salts (Wako Pure Chemical Industries, Osaka, Japan) were added to the medium of the transfected BJMC3879-Luc2 cells or to the non-transfected parental BJMC3879 cells to a final concentration of at 150 μg/ml. Expression of luciferase was confirmed in the transfected cultures by bioluminescent imaging using a Photon Imager (Biospace Lab, Paris, France).

Animals. A total of 10 female BALB/c mice at 6 weeks of age were used in this study (Japan SLC, Inc., Hamamatsu, Japan). The mice were housed no more than 5 per plastic cage on wood chip bedding with free access to water and food and maintained under conditions of controlled temperature (21±2˚C), humidity (50±10%), and lighting (12 h-12 h light-dark cycle). All were held for a 1-week acclimatization period prior to test initiation. All manipulations and treatments of the mice were performed in accordance with procedures outlined in the Guide for the Care and Use of Laboratory Animals at Osaka Medical College. At the termination of the study, all mice were euthanized under isoflurane anesthesia.

Bioluminescence imaging in vivo. While under isoflurane inhalation using an SBH Scientific anesthesia system (SBH Designs Inc., Ontario, Canada), 5×10^6 BJMC3879-Luc2 cells in 0.3 ml phosphate-buffered saline were inoculated subcutaneously into the right inguinal region of the 10 female BALB/c mice. The mice were then injected intraperitoneally with D-luciferin potassium salts (Wako Pure Chemical Industries) at 3 mg/mouse. Bioluminescence imaging with a Photon Imager (Biospace Lab) was performed weekly from weeks 2 to 10 post-inoculation. The bioluminescent signals received during the 6 min acquisition time were quantified using Photovision software (Biospace Lab). Each developing mammary tumor was measured weekly using digital calipers, and tumor volumes were calculated using the following formula: maximum diameter × (minimum diameter)^2 ×0.4 (8).

Histopathology. At necropsy, tumors and lymph nodes – routinely those from the axillary and femoral regions, as well as those appearing abnormal – were removed, fixed in 10% formaldehyde solution in phosphate buffer, and processed through to paraffin embedding. Lungs were inflated with formaldehyde solution prior to excision and immersion in fixative; the individual lobes were subsequently removed from the bronchial tree and examined for metastatic foci and similarly processed to paraffin embedding. All paraffin-embedded tissues were cut into sequential 4-μm thick sections and stained with hematoxylin and eosin for histopathological examination.

To identify lymphatic vessels in the primary mammary carcinomas, the avidin-biotin immunohistochemical complex method (LSAB kit; DakoCytomation, Carpinteria, CA, USA) was used. A hamster anti-podoplanin monoclonal antibody (AngioBio Co., Del Mar, CA, USA) against a lymphatic endothelium marker was used.

Statistical analysis. Significant differences in sequential changes in the quantitative data (tumor volumes and photon counts) were analyzed using Student's *t*-test. The quantitative data between tumor volumes and photon counts was analyzed using Pearson's correlation.

Results

Stable luciferase expression in mammary carcinoma cell line. BJMC3879luc2 cells transfected with luciferase gene showed consistent and stable luminescent signals, while parental BJMC3879 cells showed no signal. There was a strong correlation between the intensity of light emission and the cell number (data not shown).

In vivo bioluminescence imaging. Bioluminescence could be observed 2 weeks after inoculation when the tumor size reached ~20 mm^3 and we were able to determine an optimal

time point for imaging after intraperitoneal administration of luciferin by counting photons from a single tumor. The luminescent signal quickly increased and reached highest levels at 8-15 min post-injection, so we chose to image 10 min after each luciferin injection (Figure 1a).

Tumor volume steadily increased with time (Figure 1b) and the intensity of luminescent signaling showed a positive correlation with increasing tumor volume (Figure 1c; Pearson correlation r=0.95, Figure 1d). Representative sequential bioluminescent imaging in two animals is shown in Figure 2a and b; as can be seen, signals in axillary, mandibular and femoral regions were detected at 8 to 9 weeks (Figure 2a and b).

Histopathologically, the mammary carcinomas induced by BJMC3879luc2 inoculation proved to be moderately differentiated adenocarcinomas (Figure 2c). Each luminescence signal emanating from mandibular (Figure 2d), axillary (Figure 2e), femoral regions proved to be from lymph nodes (Figure 2f) histopathologically confirmed to contain metastases of the primary mammary carcinoma. However, the small metastatic foci of the lungs (Figure 2g) and ovary (Figure 2h) found at necropsy were not detected by ventral bioluminescent imaging in these cases.

Mice started to die at 8 weeks post-inoculation; only 10% survived to 10 weeks post-inoculation. Bioluminescence imaging was conducted on all surviving mice at terminal sacrifice as well as those found in moribund condition prior to euthanasia and necropsy. Figure 3a and c show the macroscopic luminescent images of animal #5 in the ventral and dorsal views, respectively. Each signal observed externally (black arrows) corresponded to macroscopically abnormal lymph nodes upon opening the abdominal cavity (black arrows, Figure 3b). In addition, macroscopically prominent vessels (as shown by the white arrows in Figure 3b) appear to correlate with external signals observed externally in Figure 3a (white arrows). We suspect that the prominent vessels are lymphatic vessels containing migrating cancer cells, since we frequently observed tumor cells within the lumina of dilated lymphatic vessels that immunohistochemically stained for podoplanin (Figure 3g), a lymphatic endothelial cell marker.

By proper positioning, we were able to detect luminescence in other cases that appeared to correlate with structures other than lymph nodes (Figure 3c-f). Histopathology confirmed metastasis to the lungs (Figure 3i), kidney (Figure 3j), and adrenals (Figure 3k) as well as to lymph nodes (Figure 3h), in animal #5. As can be seen, imaging in the abdominal position (dorsal appearance, Figure 3c) showed intense signals in areas corresponding to the kidneys and adrenals, which, macroscopically, were discolored and enlarged. Bioluminescence imaging in the dorsal position, however, did not indicate these lesions. Animal #10 showed an extensive bioluminescent signal in the abdominal region (Figure 3f) which was confirmed as liver metastasis (Figure 3l).

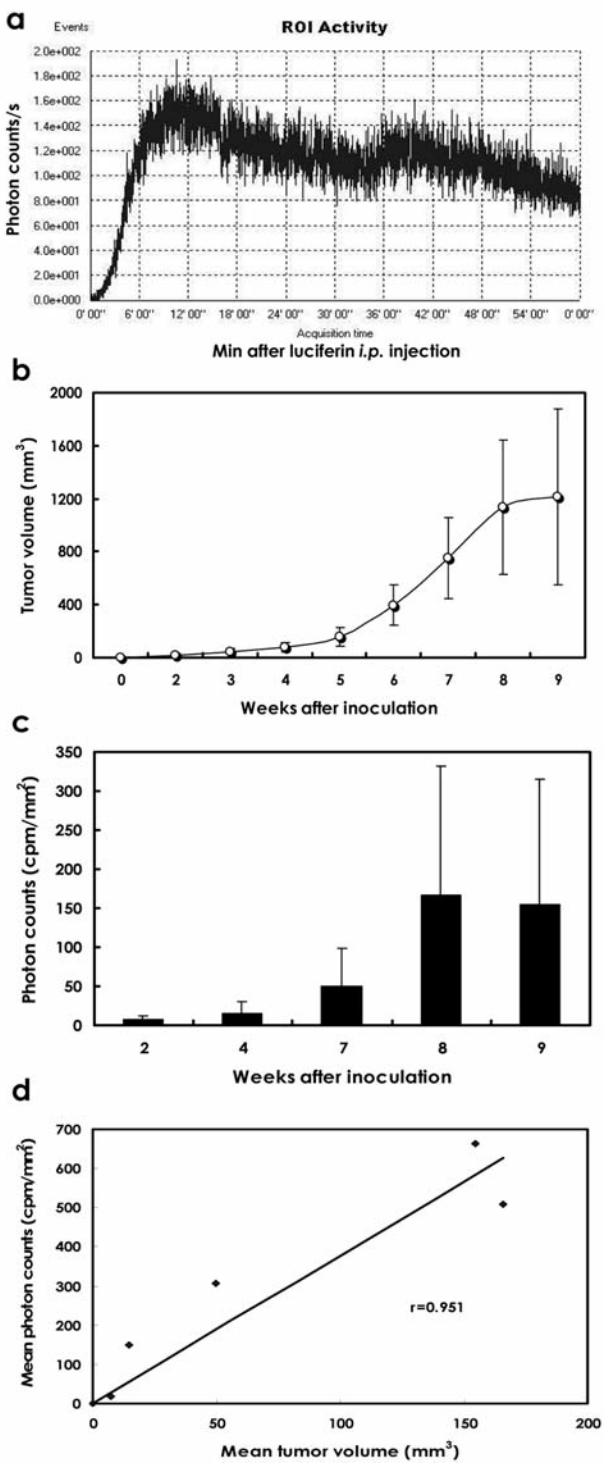

Figure 1. *a, The kinetics of photon production from a single tumor of a mouse after intraperitoneal injection with D-luciferin salts. The graph shows a peak signal 8-15 min after luciferin injection; we therefore chose to image 10 min after luciferin injections. The values plotted were integrated every 1 second. b, The relative mammary tumor volumes in female BALB/c mice. c, Histogram of the photon counts in mammary tumors from female BALB/c mice. d, Analysis of the correlation between tumor volume and photon count; Pearson's correlation r=0.95.*

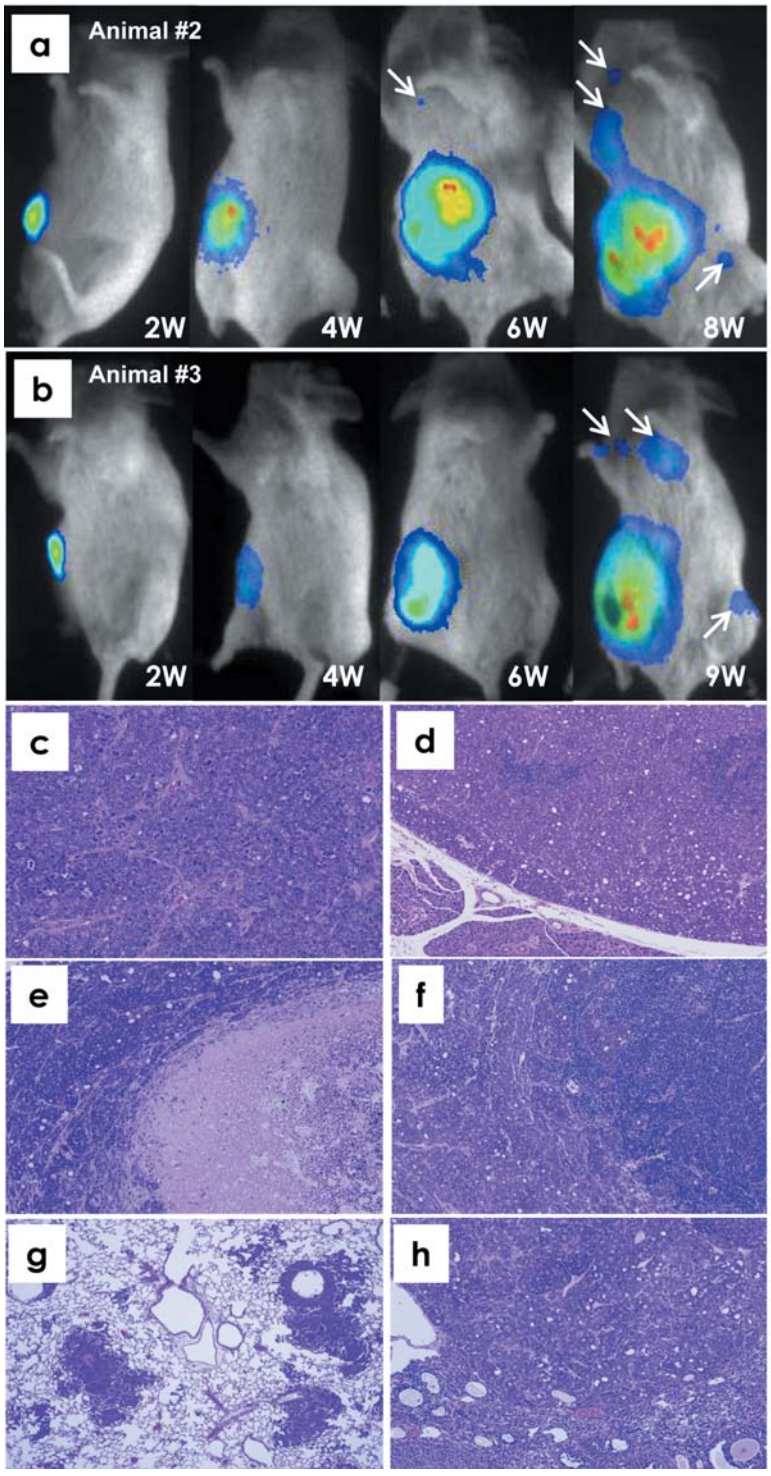

Figure 2. *a and b, Sequential bioluminescent imaging in representative individual animals. Note that the increased intensity of the bioluminescent signals correlated with increased tumor size. a, The right axillary region (arrow) showed signal at 6 weeks while the right mandibular region (arrow) and left femoral region (arrow) bioluminesced 8 weeks post-inoculation in animal #2. b, Animal #3 showed signals in both the axillary (arrows) and left femoral regions (arrow) at 9 weeks post-inoculation. c-h, Histopathologies of the primary mammary carcinoma (c, ×200) and of metastases (d-h). The primary tumor arising at the inoculation site proved to be a moderately differentiated adenocarcinoma (animal #2). Within the same mouse, metastases developed in the mandibular lymph node (d, ×100), the axillary lymph node (e, ×100), and the femoral lymph node (f, ×100) – all of which were detected in imaging in the ventral plane. However, small metastatic foci found upon necropsy in the lungs of animal #2 (g, ×40) and the ovary from animal #3 (h, ×100) were not detected in ventral bioluminescence imaging. c-h, H&E stain.*

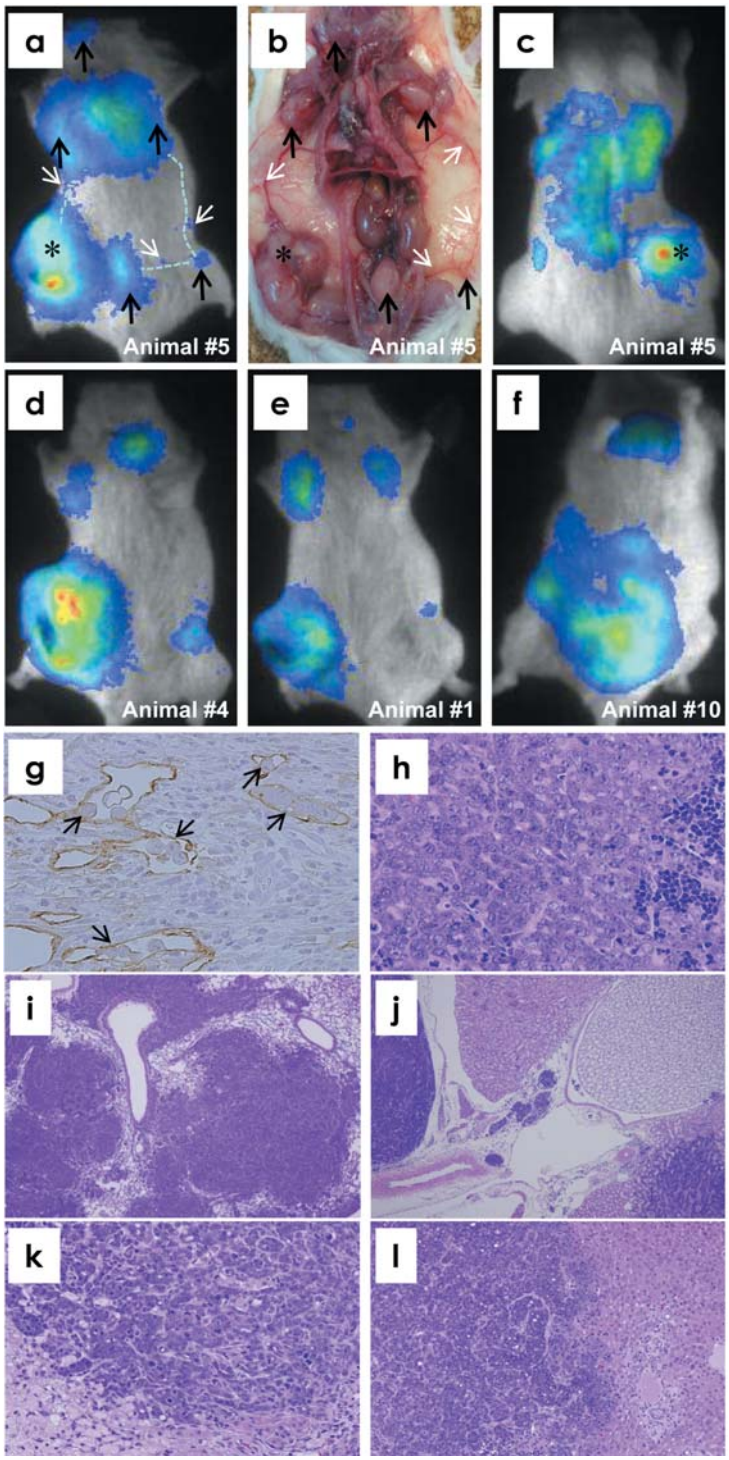

Figure 3. *a-f, Correlation of bioluminescent imaging and macroscopic and histological findings in representative mice. With animal #5 placed in the venter up position, the signals observed in regions corresponding to the primary tumor (*) and lymph nodes (a, black arrows indicate axillary, mandibular, iliac, and femoral lymph nodes) correlated to macroscopic abnormalities at necropsy findings (b, * and black arrows). Furthermore, focal signals (a, white arrows) appeared to emanate from prominent vessels observed at necropsy (b, white arrows) and may indicate tumor cells present in the lumens of distended lymphatic vessels (g, arrows, ×400) as seen with podoplanin immunohistochemistry. Dorsal imaging successfully detected macroscopic abnormalities in the kidneys and adrenals not apparent with ventral imaging of animal #5 (c); metastasis was histologically confirmed in femoral lymph nodes (h, ×400), lungs (i, ×40), kidney (j, ×40), and adrenals (k, ×200). In animals #1 and #4, luminescence was detected in areas corresponding to mandibular, axillary, and femoral lymph nodes (d and e); the large area of signal seen in animal #1 in panel f corresponded to liver metastasis (l, ×100). g, podoplanin immunohistochemistry; h-l, H&E stain.*

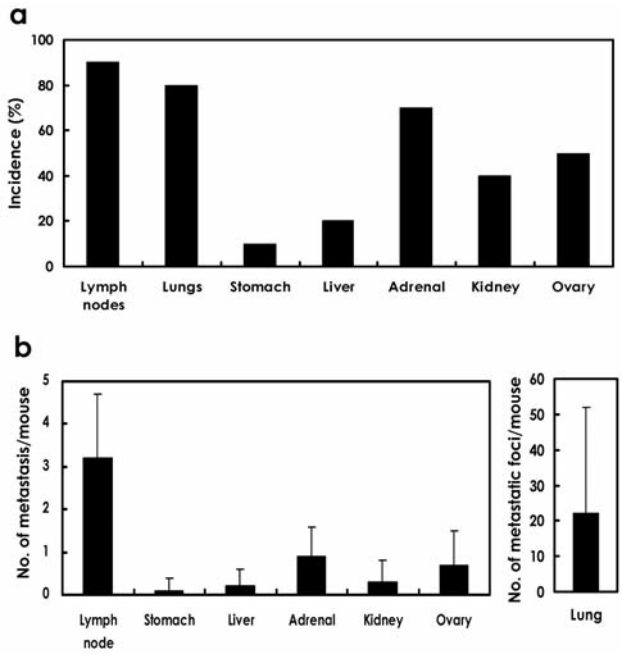

Figure 4. *The incidence of metastasis (a) and the relative numbers of metastases by organ and mouse (b) as assessed by histopathological examination. Metastatic incidence in lymph nodes, in lungs, and in adrenals was 90, 80 and 70%, respectively (a, b). The number of lung metastatic foci >250 μm in size were counted (b).*

Metastasis. Metastatic incidence and multiplicity are shown in Figure 4a and b. Metastasis to lymph nodes, lungs, and adrenals were seen in 90, 80 and 70% of mice, respectively. Metastasis to ovaries and kidneys was observed in approximately 50% of the mice. Few cases showed metastasis to either liver or stomach. The multiplicity of metastases in lymph nodes and lungs was higher than the other organs.

Discussion

Breast cancer poses a major health problem worldwide, with the major cause of death from the disease due to metastasis. Lymph node metastasis is, in fact, one of the most significant adverse prognostic factors for breast cancer survival (9). In breast cancer surgery, dissection of the axillary lymph nodes is considered the standard of care for performing staging and achieving local control (10); sentinel lymph node biopsy has become a standard procedure for patients with no evidence of metastasis to the axillary lymph nodes to avoid unnecessary dissection (10).

Similar to the scenario in the human disease, the mouse mammary cancer model used in this study showed a high metastatic propensity to lymph nodes, especially to axillary and femoral lymph nodes, the latter corresponding to the human inguinal nodes. We found that bioluminescence signals were detectable at an early time point in lymph node metastasis, and suspect that bioluminescence imaging may actually be able to show micrometastasis (cancer cells migrating in the lymphatic vessels). In therapeutic studies using animal cancer models, therapeutic effects are usually assessed by sequential tumor volume and endpoint parameters such as survival time and histopathological analysis. The advantage of this cancer model in biomedical research is that of being able to obtain sequential information concerning the presence of metastases and metastatic location in living animals; using bioluminescence imaging, it is possible to monitor tumor growth, to detect cancer metastasis at an early time point, and to quantify therapeutic efficacy *in vivo* over time. Another asset to this model is its simplicity, and using luciferase overcomes the problems with autofluorescence seen with such agents as GFP. Furthermore, the number of animals used can be greatly reduced while increasing the extent of data. We believe this model can be used as a quantifiable and reliable mammary cancer model that can be employed in many cancer gene therapy and pharmacological studies.

Acknowledgements

This investigation was supported by a Grant-in-Aid for Scientific Research (C)(2) from the Ministry of Education, Culture, Sports, Science and Technology (MEXT) of Japan (No. 19591520 to M.A. Shibata) and, in part, from a High-Tech Research Center Grant to Osaka Medical College from MEXT. We also thank Ms. Deborah Devor-Henneman (Ohio State University of Veterinary Medicine, OH, USA) for critical review of the manuscript, Mr. Tetsuya Sonoyama (Sowa Trading Co., Inc., Osaka, Japan) for technical assistance with bioluminescent imaging and Ms. Mika Yoshida for excellent secretarial assistance.

References

1 le Masne de Chermont Q, Chaneac C, Seguin J, Pelle F, Maitrejean S, Jolivet JP, Gourier D, Bessodes M and Scherman D: Nanoprobes with near-infrared persistent luminescence for *in vivo* imaging. Proc Natl Acad Sci USA *104*: 9266-9271, 2007.

2 Bhaumik S and Gambhir SS: Optical imaging of Renilla luciferase reporter gene expression in living mice. Proc Natl Acad Sci USA *99*: 377-382, 2002.

3 Jemal A, Siegel R, Ward E, Hao Y, Xu J, Murray T and Thun MJ: Cancer stastics, 2008. CA Cancer J Clin *58*: 71-96, 2008.

4 Morimoto J, Imai S, Haga S, Iwai Y, Iwai M, Hiroishi S, Miyashita N, Moriwaki K and Hosick HL: New murine mammary tumor cell lines. In Vitro Cell Dev Biol *27A*: 349-351, 1991.

5 Shibata MA, Morimoto J and Otsuki Y: Suppression of murine mammary carcinoma growth and metastasis by HSV*tk*/GCV gene therapy using *in vivo* electroporation. Cancer Gene Ther *9*: 16-27, 2002.

6 Shibata MA, Ito Y, Morimoto J and Otsuki Y: Lovastatin inhibits tumor growth and lung metastasis in mouse mammary carcinoma model: a p53-independent mitochondrial-mediated apoptotic mechanism. Carcinogenesis *25*: 1887-1898, 2004.

7 Shibata MA, Ito Y, Morimoto J, Kusakabe K, Yoshinaka R and Otsuki Y: *In vivo* electrogene transfer of interleukin-12 inhibits tumor growth and lymph node and lung metastases in mouse mammary carcinomas. J Gene Med *8*: 335-352, 2006.

8 Shibata MA, Liu M-L, Knudson MC, Shibata E, Yoshidome K, Bandy T, Korsmeyer SJ and Green JE: Haploid loss of bax leads to accelerated mammary tumor development in C3(1)/SV40-TAg transgenic mice: reduction in protective apoptotic response at the preneoplastic stage. EMBO J *18*: 2692-2701, 1999.

9 Cody HS 3rd, Borgen PI and Tan LK: Redefining prognosis in node-negative breast cancer: can sentinel lymph node biopsy raise the threshold for systemic adjuvant therapy? Ann Surg Oncol *11*: 227S-230S, 2004.

10 Veronesi U, Paganelli G, Viale G, Luini A, Zurrida S, Galimberti V, Intra M, Veronesi P, Maisonneuve P, Gatti G, Mazzarol G, De Cicco C, Manfredi G and Fernandez JR: Sentinel-lymph-node biopsy as a staging procedure in breast cancer: update of a randomised controlled study. Lancet Oncol *7*: 983-990, 2006.

Received July 6, 2009
Revised October 22, 2009
Accepted October 23, 2009